ISSN 1063-7826, Semiconductors, 2012, Vol. 46, No. 10, pp. 1316–1320. © Pleiades Publishing, Ltd., 2012.
Original Russian Text © V.V. Kabanov, Ye.V. Lebiadok, G.I. Ryabtsev, A.S. Smal, M.A. Shchemelev, D.A. Vinokurov, S.O. Slipchenko, Z.N. Sokolova, I.S. Tarasov, 2012, published in Fizika i Tekhnika Poluprovodnikov, 2012, Vol. 46, No. 10, pp. 1339–1343.

PHYSICS OF SEMICONDUCTOR DEVICES

Radiative and Nonradiative Recombination in the Active Layers of High-Power InGaAs/GaAs/AlGaAs Laser Diodes

V. V. Kabanov[a], Ye. V. Lebiadok[a], G. I. Ryabtsev[a], A. S. Smal[a], M. A. Shchemelev[a], D. A. Vinokurov[b], S. O. Slipchenko[b]^, Z. N. Sokolova[b], and I. S. Tarasov[b]

[a] *Stepanov Institute of Physics, National Academy of Sciences of Belarus, Minsk, 220072 Belarus*

[b] *Ioffe Physical–Technical Institute, Russian Academy of Sciences, St. Petersburg, 194021 Russia*

^e-mail: sergHPL@mail.ioffe.ru

Submitted March 28, 2012; accepted for publication, April 2, 2012

Abstract—Recombination rates due to radiative and nonradiative processes and the rate of recombination induced by amplified luminescence have been determined for lasers based on an asymmetric InGaAs/GaAs/AlGaAs heterostructure with an ultrawide waveguide in the subthreshold region. It is shown that the quantum efficiency of luminescence is no less than 91.5% for the laser samples studied.

DOI: 10.1134/S1063782612100077

1. INTRODUCTION

In lasers based on an asymmetric InGaAs/GaAs/AlGaAs heterostructure with an ultrawide waveguide, powers of about 16 W can be reached in the continuous-wave (CW) lasing mode and 145 W in the pulsed mode [1–4]. To raise the power further, it is important, together with using the conventional approach in which the internal optical loss is reduced [1–5], to study in more detail the possible loss channels of the pump energy, such as the nonradiative recombination and amplified luminescence (superluminescence) important in the subthreshold region.

The goal of our study was to examine the loss channels associated with nonradiative recombination in InGaAs/GaAs/AlGaAs lasers and to analyze the amplified luminescence.

2. EXPERIMENTAL AND CALCULATED LASER EMISSION SPECTRA

In our experiments, we measured the threshold current and front-face emission spectra of lasers with an ultrawide waveguide, based on a double InGaAs/GaAs/AlGaAs heterostructure with a single strained InGaAs quantum well (QW), developed at the Ioffe Physical–Technical Institute, Russian Academy of Sciences. In the asymmetric heterostructure with an ultrawide waveguide with a total thickness of 1.7 μm, the active layer was shifted by 0.2 μm toward the *p* emitter. The parameters of the heterostructure and laser are listed in Tables 1 and 2 and presented in Fig. 1.

We studied lasers with a lasing wavelength of $\lambda_{las} = 1060$ nm and threshold current of $I_{th} = 670$ mA at the ambient temperature $T = 295$ K.

Figure 2 shows the front-face emission spectra of the lasers in the subthreshold mode at pump currents of 100 to 670 mA.

The experimentally measured emission spectra (in relative units of intensity), generation wavelength, and full internal optical loss coefficient, found from the light–current characteristics of a laser, make it possible to determine the radiative recombination rate in absolute units [6, 7].

Table 1. Composition of the heterostructure layers of the laser under study

Heterostructure layer	Layer composition	Layer thickness	Dopant concentration, 10^{18} cm^{-3}
Contact	GaAs	0.2 μm	3.5
p emitter	$Al_{0.3}Ga_{0.7}As$:Mg	1.5 μm	3.5
Waveguide	GaAs	0.65 μm	Undoped
Active	$In_xGa_{1-x}As$	9 nm	Undoped
Waveguide	GaAs	1.05 μm	Undoped
n emitter	$Al_{0.3}Ga_{0.7}As$:Si	2.0 μm	1.0
Substrate	GaAs	100 μm	1.0

For lasers with a QW active layer, the spontaneous emission intensity $W_{sp}(h\nu)$ and the gain $g(h\nu)$ spectra are given by the expressions [8, 9]:

$$W_{sp}(h\nu) = \frac{8\pi n^2 (h\nu)^3}{c^2 h^3}\left[1 - \exp\left(\frac{h\nu - \Delta F}{kT}\right)\right]^{-1} g(h\nu), \quad (1)$$

where n is the refractive index of the active layer; h is Planck's constant; ν is the emission wavelength; c is the speed of light in free space; $\Delta F = F_e - F_h$ is the difference between the quasi-Fermi levels for electrons (F_e) and holes (F_h), found from the quasineutrality equation; $g(h\nu)$ is the gain spectrum in the QW of the active region, calculated within the spectral model without performing the selection rule over the wave vector,

$$g(h\nu) = \frac{32e^2 a_0^2 \pi^2 m_e m_h kT|\mathbf{M}|^2}{\varepsilon_0 m_0^2 h^3 cndh\nu} \times \sum_i H(h\nu - (E_g + E_{ci} + E_{hi})) \times \ln\left\{\frac{1 + \exp[(F_e - E_g - E_{ci})/kT]}{1 + \exp[(h\nu + F_h - E_g - E_{ci})/kT]} \times \frac{1 + \exp[(-E_{hi} - F_h)/kT]}{1 + \exp[(h\nu - E_{hi} - F_e)/kT]} \exp\left(\frac{h\nu - \Delta F}{kT}\right)\right\}. \quad (2)$$

Here, $a_0 = 1.7 \times 10^{-9}$ m is the Bohr radius; m_e and m_h are the effective masses of electrons in the conduction band and heavy holes in the valence band [10]; m_0 is the free electron mass; e is the elementary charge; ε_0 is the permittivity of free space; d is the thickness of the active region; E_g is the band-gap width; E_{ci} and E_{hi} are the energy levels for electrons in the conduction band and heavy holes in the valence band; and H is the Heaviside function. All the parameters refer to the active region. The gain spectrum is calculated in the approximation of parabolic bands. Because of the low values of the threshold concentration of nonequilibrium carriers, $n_{th} = 2.5 \times 10^{18}$ cm^{-3}, for the lasers under study, the concentration-related changes in the density of states and in the dispersion relations were disregarded [11]. $|\mathbf{M}|^2$ is the squared matrix element of the band-to-band optical transitions, averaged over the polarizations and directions of radiation propagation. We regarded $|\mathbf{M}|^2$ as a fitting parameter when determining the absolute value of $g(h\nu)$. The value of $|\mathbf{M}|^2$ depends

Table 2. Parameters of the layer under study

Parameter	Parameter value
Cavity length L	2.8 mm
Stripe-contact width w	100 μm
Active-layer thickness d	9 nm
Rear-mirror reflectance R_1	95%
Front-mirror reflectance R_2	4%
Refractive index n of the active layer	3.89
Internal optical-loss coefficient ρ	0.5 cm^{-1}
Optical confinement factor Γ for the main mode in the active layer	0.0072

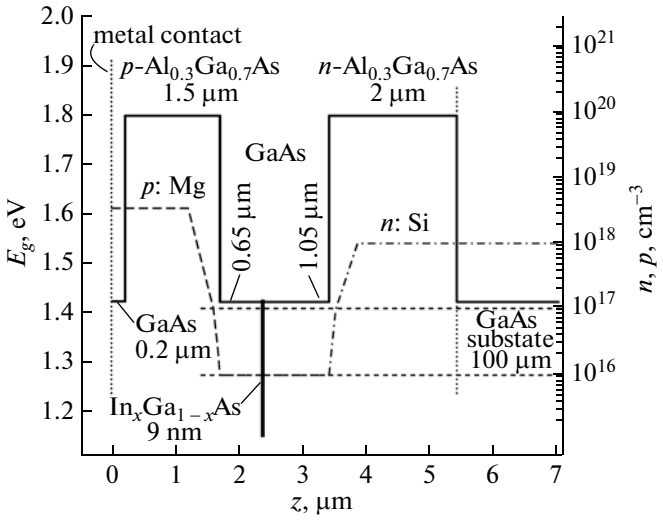

Fig. 1. Band diagram and doping profile of the heterostructure layers of the laser under study. E_g is the band gap; n and p are the electron and hole concentrations; and z is the coordinate in the layer growth direction.

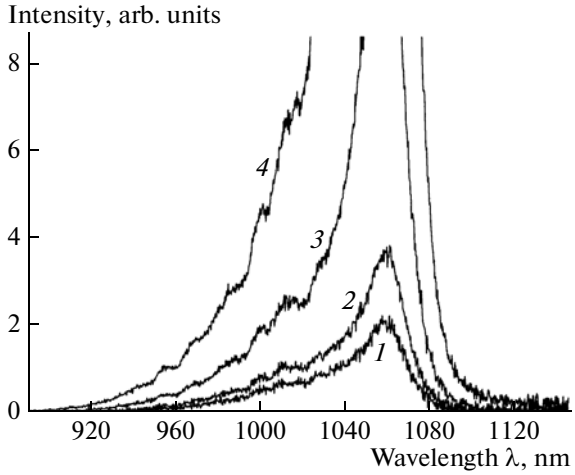

Fig. 2. Front-mirror emission spectra of the laser at injection currents: (*1*) 100, (*2*) 250, (*3*) 400, and (*4*) 670 mA

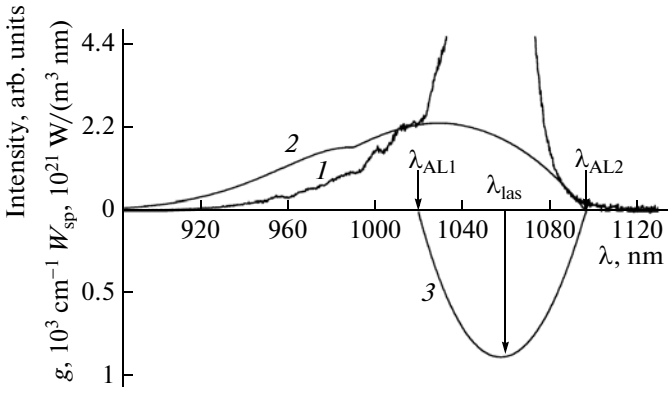

Fig. 3. (*1*) Experimental front-face emission spectrum of the laser and calculated spectra of (*2*) spontaneous emission W_{sp} and (*3*) gain g at a threshold pump current of 670 mA.

on the photon energy [11]. We found that $|\mathbf{M}|^2 = 2.1 \times 10^{-49}$ kg^2 m^2 s^{-2} for the InGaAs/GaAs/AlGaAs laser samples under study.

Calculation of the luminescence and gain spectra by formulas (1) and (2) is difficult because there are no reliable experimental data on the band-gap width and, consequently, on the energy-level positions in the strained InGaAs QW in the laser samples under study. However, based on these formulas, we can construct a number of luminescence and gain spectra in relative units, by varying (within reasonable limits) the band-gap width of InGaAs. The closest to the true E_g will be that value at which the gain has a maximum at the lasing wavelength λ_{las} (Fig. 3). At the lasing threshold, the modal gain $\Gamma g(\lambda_{las})$ is equal to the total loss in the laser, k_{tot}, i.e., $\Gamma g(\lambda_{las}) = k_{tot}$, where Γ is the optical confinement factor. The total loss is constituted by the full internal loss ρ and the mirror loss: $k_{tot} = \rho + (1/2L)\ln(1/R_1R_2)$, where L is the laser-cavity length, and R_1 and R_2 are the mirror reflectances. The luminescence and gain spectra in relative units can be represented in absolute units by using (1) and (2). (For the maximum gain, we take the value equal to the total emission loss with consideration for the optical confinement factor, k_{tot}/Γ. This enables renormalization of the whole gain spectrum. We calculate the luminescence spectrum in absolute units in accordance with (1), using the obtained gain spectrum in absolute units.)

The spontaneous luminescence spectrum in absolute units makes it possible to calculate the radiative recombination rate R_{sp}:

$$R_{sp} = \int_{h\nu_1}^{h\nu_2} \frac{W_{sp}(h\nu)}{h\nu} d(h\nu), \quad (3)$$

where ν_1 and ν_2 are the boundary frequencies of the spontaneous emission spectrum.

The front-face emission spectrum (curve *1*, relative units) and calculated spectra of spontaneous emission (curve *2*, W m^{-3} nm^{-1} units) and gain (curve *3*, cm^{-1} units) at a threshold current of 670 mA are shown in Fig. 3. The wavelength range from λ_{AL1} to λ_{AL2} (spectral range of positive gain values) (see curve *3*) is that of amplified luminescence. It is known [12] that the "excess" emission in the subthreshold range of pump currents is due to amplified luminescence appearing at frequencies at which the gain $g(h\nu)$ is positive but is lower than the total loss in the laser, i.e., $0 < g(h\nu) < k_{tot}$. Thus, it follows from Fig.3 that an amplified luminescence band is observed in the emission spectrum of the laser. The volume-average spectral density of the amplified-luminescence flux, $S_{AL}(h\nu)$, can be calculated by the expression [13]

$$S_{AL}(h\nu) = \frac{W_{sp}(h\nu)}{k_{AL} - \Gamma g(h\nu)}, \quad (4)$$

where k_{AL} is the amplified-luminescence loss coefficient. The loss coefficient k_{AL} determines the loss for the amplified-luminescence flux, averaged over the solid angle and emission spectrum [14–17]. It was shown in [14–17] that the inequality $\rho < k_{AL} < k_{tot}$ is observed for the amplified-luminescence loss coefficient.

The rate of recombination induced by amplified luminescence is given by

$$R_{AL} = \int \frac{\Gamma g(h\nu) S_{AL}(h\nu)}{h\nu} d(h\nu). \quad (5)$$

The integration in (5) is over the spectral range in which the gain is positive.

It follows from (4) that, in a certain frequency range (near the maximum gain), the denominator can take rather small values. According to (5), this leads to a significant increase in the rate and, consequently, in the intensity of amplified luminescence in this frequency range.

In [14], the following dependence of the loss coefficient k_{AL} on the active-layer area S_{pn} was obtained:

$$k_{AL} = \frac{\Delta}{\sqrt{S_{pn}}}, \quad (6)$$

where Δ is the proportionality factor. It can be found from the results of [14–17] that $\Delta = 0.2$ for the laser samples we studied.

3. RESULTS AND DISCUSSION

Following the approach described above, we calculated the radiative recombination rate: $R_{sp} = 1.3 \times$

10^{27} cm^{-3} s^{-1}. Substituting this value of R_{sp} and the threshold carrier concentration $n_{th} = 2.5 \times 10^{18}$ cm^{-3} into the expression for the spontaneous recombination rate $R_{sp} = Bn_{th}^2$, we obtain for the spontaneous recombination coefficient the value $B = 2.1 \times 10^{-10}$ cm^2 s^{-1}, which is close to its values for GaAs [18, 19] and InGaAs [20].

The rate of recombination induced by amplified luminescence, calculated by formulas (4)–(6), is an order of magnitude lower than the spontaneous recombination rate R_{sp}: $R_{AL} = 1.0 \times 10^{26}$ cm^{-3} s^{-1}, although formulas (4) and (5) contain a small denominator, compared with formula (3). The reason is that, in contrast to formula (3), integration in formula (5) is only within the gain band, rather than over the entire spontaneous emission spectrum.

The values of the rates R_{sp} and R_{AL} at the lasing threshold make it possible to determine the recombination rate Q due to nonradiative transitions [6]:

$$\sigma j_{th} = ed(R_{sp} + Q + R_{AL}), \quad (7)$$

where j_{th} is the threshold injection current; e is the elementary charge; d is the active-layer thickness; and σ is the parameter taking into account current spreading.

The threshold injection current density j_{th} was found for the samples under study from the experimentally measured value of the threshold current I_{th}. When determining the nonradiative recombination rate, we took into account the current spreading effect in the layers of the laser diode heterostructures [12]. For the lasers under study, carrier spreading into passive regions of the laser leads to an 8% decrease in the injection current density beneath the stripe contact, i.e., $\sigma = 0.92$ (it is assumed that current spreading occurs in the 0.2-μm-thick emitter layer that has a resistivity of 1.0×10^{-1} Ω cm).

Substituting values of the rates R_{sp} and R_{AL} into relation (7), we obtain for the nonradiative recombination rate a value of $Q = 1.2 \times 10^{26}$ cm^{-3} s^{-1}. If we assume that Auger recombination is the main nonradiative process, then we obtain, using the relation $Q = Cn_{th}^3$, a value of 7.6×10^{-30} cm^6 s^{-1} for the Auger recombination coefficient C, which is in good agreement with the data for GaAs [18, 21] and InGaAs [20].

The radiative and nonradiative recombination rates determine the internal quantum efficiency of luminescence, η [7]:

$$\eta = \frac{R_{sp}}{R_{sp} + Q}. \quad (8)$$

In the laser diode samples under study, the quantum efficiency of luminescence is 91.5%.

Figure 4 shows the spectra of spontaneous emission (curve *1*) and amplified luminescence (curve *2*), calculated by formulas (1), (2), and (4), and the experimentally recorded spectrum of the emission from the front face of the laser cavity (curve *3*) at a threshold pump current of 670 mA. The calculated spontaneous-emission and amplified-luminescence spectra were integrated over the volume of the active region. It follows from Fig. 4 that, in the frequency range in which the gain $g(h\nu)$ is positive, the intensity of amplified luminescence exceeds that of spontaneous emission. This is indicative of the high quality of the laser heterostructure under study, in which the real ratio between the gain and total loss exceeds that taken into account in calculations. Here, the nonradiative recombination rate found from relation (7) must be smaller than the value we obtained, $Q = 1.2 \times 10^{26}$ cm^{-3} s^{-1}, which will lead to an increase in the internal quantum efficiency of luminescence. Thus, the value $\eta = 91.5\%$ can be regarded as the lower limit for the internal quantum efficiency of luminescence for the lasers studied.

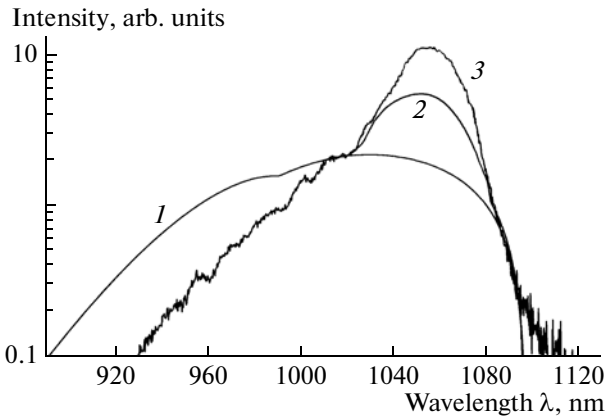

Fig. 4. Calculated spectra of (*1*) spontaneous emission and (*2*) amplified luminescence and (*3*) experimentally recorded emission from the front face of the laser cavity at a threshold pump current of 670 mA.

4. CONCLUSIONS

Recombination rates due to radiative and nonradiative processes and amplified luminescence were determined for lasers based on an asymmetric InGaAs/GaAs/AlGaAs heterostructure with an ultrawide waveguide.

It was shown that the quantum efficiency of luminescence is no less than 91.5% for the laser samples studied. To determine the recombination rates, including recombination induced by the amplified luminescence more precisely, it is necessary to fabricate special small-size heterostructure samples with matted facets.

It should be noted that, when analyzing the loss channels of the laser excitation energy, it is necessary to take into account that, with the injection current increasing to above the threshold value, stable closed

modes can contribute to the pumping energy loss, together with the amplified-luminescence flux [22].

REFERENCES

1. S. O. Slipchenko, D. A. Vinokurov, N. A. Pikhtin, Z. N. Sokolova, A. L. Stankevich, I. S. Tarasov, and Zh. I. Alferov, Semiconductors **38**, 1430 (2004).
2. S. O. Slipchenko, Z. N. Sokolova, N. A. Pikhtin, K. S. Borshchev, D. A. Vinokurov, and I. S. Tarasov, Semiconductors **40**, 990 (2006).
3. I. S. Tarasov, N. A. Pikhtin, S. O. Slipchenko, Z. N. Sokolova, D. A. Vinokurov, K. S. Borschev, V. A. Kapitonov, M. A. Khomylev, A. Yu. Leshko, A. V. Lyutetskiy, and A. L. Stankevich, Spectrochim. Acta A **66**, 819 (2007).
4. I. S. Tarasov, Quantum Electron. **40**, 661 (2010).
5. D. A. Livshits, I. V. Kochnev, V. M. Lantratov, N. N. Ledentsov, T. A. Nalyot, I. S. Tarasov, and Zh. I. Alferov, Electron. Lett. **36**, 1848 (2000).
6. L. I. Burov, E. V. Lebedok, V. K. Kononenko, A. G. Ryabtsev, and G. I. Ryabtsev, J. Appl. Spectrosc. **74**, 878 (2007).
7. V. V. Kabanov, E. V. Lebiadok, A. G. Ryabtsev, G. I. Ryabtsev, M. A. Shchemelev, V. V. Sherstnev, A. P. Astakhova, and Yu. P. Yakovlev, Semiconductors **43**, 500 (2009).
8. P. T. Landsberg, M. S. Abrahams, and M. Osinski, IEEE J. Quant. Electron. **21**, 24 (1985).
9. A. A. Afonenko, V. K. Kononenko, I. S. Manak, and V. A. Shevtsov, Semiconductors **31**, 929 (1997).
10. M. P. Krijn, Semicond. Sci. Technol. **6**, 27 (1991).
11. L. A. Coldren and S. W. Corzine, *Diode Lasers and Photonicintegrated Circuits* (Wiley, New York, 1995).
12. H. C. Casey and M. B. Panish, *Heterostructure Lasers* (Academic Press, New York, 1978; Mir, Moscow, 1981), pt B.
13. V. P. Gribkovskii, *Theory of Absorption and Emission of Light in Semiconductors* (Nauka Tekhnika, Minsk, 1975) [in Russian].
14. V. K. Kononenko and V. P. Gribkovskii, Sov. Phys. Semicond. **5**, 1631 (1971).
15. L. I. Burov, I. N. Varaksa, S. V. Voitikov, M. I. Kramar, A. G. Ryabtsev, and G. I. Ryabtsev, Quantum Electron. **32**, 260 (2002).
16. G. I. Ryabtsev and A. S. Smal', J. Appl. Spectrosc. **70**, 550 (2002).
17. G. I. Ryabtsev, T. V. Bezyazychnaya, M. V. Bogdanovich, V. V. Parastchuk, A. I. Yenzhyieuski, L. I. Burov, A. S. Gorbatsevich, A. G. Ryabtsev, M. A. Shchemelev, V. V. Bezotosnyi, K. A. Shore, and S. Banerjee, Appl. Phys. B **90**, 471 (2008).
18. G. R. Hadley, J. P. Hohimer, and A. Owyoung, IEEE J. Quant. Electron. **24**, 2138 (1988).
19. Z. N. Sokolova and V. B. Khalfin, Sov. Phys. Semicond. **23**, 1117 (1989).
20. L. V. T. Nguyen and P. C. R. Gurnev, IEEE J. Sel. Top. Quantum Electron. **1**, 494 (1995).
21. B. L. Gel'mont and Z. N. Sokolova, Sov. Phys. Semicond. **16**, 1067 (1982).
22. S. O. Slipchenko, A. A. Podoskin, N. A. Pikhtin, Z. N. Sokolova, A. Yu. Leshko, and I. S. Tarasov, Semiconductors **45**, 663 (2011).

Translated by M. Tagirdzhanov